ACS Synthetic Biology

pubs.acs.org/synthbio Research Article

Leveraging Synthetic Antibody−DNA Conjugates to Expand the CRISPR-Cas12a Biosensing Toolbox

Published as part of ACS Synthetic Biology special issue "Diagnostics".

Elisa Paialunga, Neda Bagheri, Marianna Rossetti, Laura Fabiani, Laura Micheli, Alejandro Chamorro-Garcia,* and Alessandro Porchetta*

Cite This: https://doi.org/10.1021/acssynbio.4c00541 Read Online

ACCESS | Metrics & More | Article Recommendations | Supporting Information

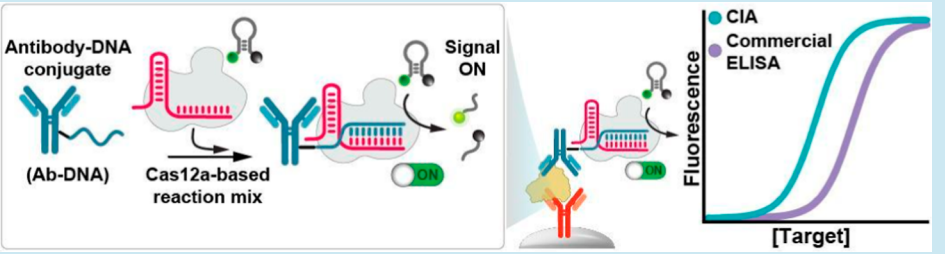

ABSTRACT: We report here the use of antibody−DNA conjugates (Ab−DNA) to activate the collateral cleavage activity of the CRISPR-Cas12a enzyme. Our findings demonstrate that Ab−DNA conjugates effectively trigger the collateral cleavage activity of CRISPR-Cas12a, enabling the transduction of antibody-mediated recognition events into fluorescence outputs. We developed two different immunoassays using an Ab-DNA as activator of Cas12a: the CRISPR-based immunosensing assay (CIA) for detecting SARS-CoV-2 spike S protein, which shows superior sensitivity compared with the traditional enzyme-linked immunosorbent assay (ELISA), and the CRISPR-based immunomagnetic assay (CIMA). Notably, CIMA successfully detected the SARS-CoV-2 spike S protein in undiluted saliva with a limit of detection (LOD) of 890 pM in a 2 h assay. Our results underscore the benefits of integrating Cas12a-based signal amplification with antibody detection methods. The potential of Ab−DNA conjugates, combined with CRISPR technology, offers a promising alternative to conventional enzymes used in immunoassays and could facilitate the development of versatile CRISPR analytical platforms for the detection of non-nucleic acid targets.

KEYWORDS: *CRISPR-Cas12a, collateral cleavage, trans-cleavage, antibody−DNA conjugate, immunoassay, fluorescence*

1. INTRODUCTION

In the rapidly advancing field of biosensing, the CRISPR-based systems have emerged as a versatile and powerful bionanotechnological tool. These systems leverage the specific and programmable nature of CRISPR-Cas enzymes to enable the highly sensitive and accurate detection of various biological targets. To date, the widespread use of CRISPR technology for biosensing applications has been mainly driven by the identification of collateral cleavage nuclease activity (i.e., trans-cleavage) of CRISPR type V (Cas12 and Cas14) and VI (Cas13) enzymes.[1] They offer an optimal toolkit for (bio)molecular detection given their capability of target recognition, signal transduction, and signal amplification in one step,[2−5] with applications in molecular diagnostics,[6−8] pathogen detection,[9,10] and genetic screening.[11,12] Besides the enhanced sensitivity, one of the main advantages of combining target recognition and CRISPR-based amplification into a single recognition/transducer entity is the simplification of detection platforms. The integration results in a minimal number of reagents and reaction steps, significantly enhancing the efficiency and ease of use. Furthermore, this feature facilitates seamless incorporation into activity-based sensors, which utilize catalytic activity for sensing, measuring, or reporting on disease states,[13,14] as well as for bioimaging of disease cells.[15] These versatile features have spurred a rising trend of research activities that take advantage of CRISPR-Cas systems, particularly for the detection of nucleic acids[1,4,16,17] even in multiplexed[18−20] assay formats.

Nonetheless, there is a pressing need to expand the application of CRISPR-Cas-based detection beyond its conventional focus on nucleic acids (NA).[21−24] Achieving this, however, is molecularly challenging due to the difficulty of converting the recognition of non-nucleic acid targets into a

Received: August 9, 2024
Revised: December 17, 2024
Accepted: December 19, 2024

trigger for CRISPR-Cas activity. This can be achieved by engineering mechanisms that enable a functional nucleic acid to bind the Cas/RNA complex only after interacting with the target molecule, for instance, using switchable DNA/RNA elements that change conformation in response to target binding. In this respect, molecular mechanisms relying on the target-induced sequestration or release of a nucleic acid input upon binding (such as an aptamer or short nucleic acid sequence) have been developed to control the activation of CRISPR-Cas systems.[25−27] These approaches, however, present limitations related to signal leak given the competition of the functional nucleic acid with the target and crRNA. In addition, engineering precise on−off molecular switching is not trivial and easy to generalize, particularly with RNA-based receptors that can populate multiple conformations. Other strategies such as those based on proximity-based activation[28] require the simultaneous binding of the target molecule to recognition elements that are bioconjugated to a nucleic acid scaffold. These approaches face limitations in their generalizability to different targets due to their requirement for dual concomitant binding onto two distinct binding sites of the same target molecule.[29,30] In general, CRISPR assays for non-NA targets require multistep analysis due to competitive binding, and the background signal can compromise sensitivity and accuracy. These factors collectively have hindered their application in field or point-of-care diagnostics.

Antibodies offer well-established advantages for biomolecular analysis including high affinity and specificity for the target, the ability to detect virtually any target, and the wide chemical toolbox for their conjugation[31] to other biological species such as nucleic acids,[32] peptides and enzymes, or synthetic molecules (i.e., drugs, isotopes, or organic molecules). This has allowed the development of a portfolio of biotechnological applications that take advantage of antibody-based systems. Among them, synthetic antibody−DNA conjugates (Ab−DNA) have gained the attention of the scientific community as they combine the high-affinity binding properties of antibodies with the large variety of functionalities of synthetic DNA.[32] One typical application involves utilizing Ab−DNA conjugates as recognition elements, triggering enzyme-based nucleic acid amplification upon target detection. Therefore, DNA-tagged antibodies have demonstrated considerable efficacy in diverse applications, including proximity ligation assays,[32,33] immuno-PCR,[34] and targeted drug delivery.[35] They have also found utility in fluorescence microscopy, DNA-PAINT imaging, and protein-templated reactions.[36−38] More recently, Ab−DNA complexes obtained through biotin−streptavidin chemistry have also been adapted into CRISPR-based immunoassays for the detection of protein targets.[39−42] However, the antibody functionalization through biotin−streptavidin chemistry has been reported to decrease the expected analytical sensitivity of the CRISPR-based assay.[41] This reduction is primarily due to increased steric hindrance caused by streptavidin, which interferes with the recognition and binding efficiency of the Cas13a/crRNA complex. As a result, nucleic acid preamplification is still required to achieve the subpicomolar detection limits, at the cost of a longer and reagent-intensive analytical procedure.

Hereby, we report the development of immunoassays utilizing synthetic an Ab−DNA conjugate to directly activate the collateral cleavage activity of CRISPR-Cas12a (Figure 1A). This approach combines the high-affinity targeting of proteins, via the antibody, and fluorescence signal amplification via

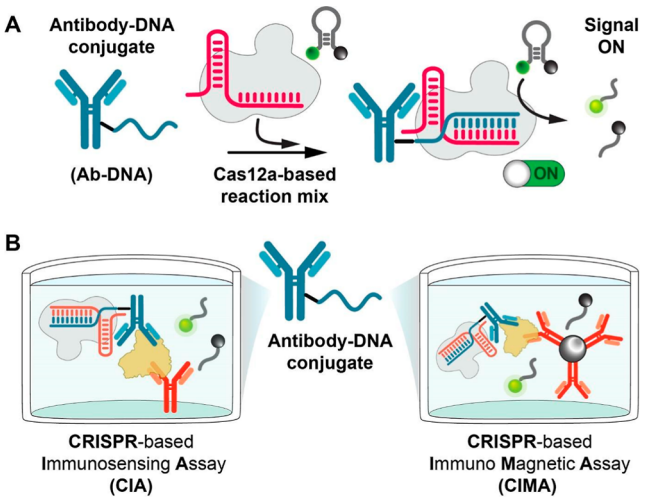

Figure 1. Schematic description of the CRISPR-Cas12a-based detection using the antibody−DNA (Ab−DNA) conjugate. (A) The DNA sequence covalently attached to the antibody is designed to hybridize with the complementary crRNA sequence of the CRISPR-Cas12a complex (ribonucleoprotein complex, RNP). This recognition event triggers the collateral cleavage activity of Cas12a, resulting in a fluorescence signal increase as the output of the digestion of the FRET-based DNA reporter. (B) On the left, a schematic description of a CRISPR-based immunosorbent assay (CIA) and, on the right, a magnetic bead-based sandwich assay (CRISPR-based immunomagnetic assay, CIMA).

Cas12a-based collateral cleavage. The assay does no require the addition of a reactive substrate (e.g., TMB, 2,4-dinitrophenol, ABTS, etc.) for signal generation as the CRISPR reaction mix already contains the DNA reporter probe. In our study, we first characterized the collateral nuclease activity of Cas12a triggered by antibody−DNA (Ab−DNA) conjugates. Next, to illustrate the versatility of this approach, we developed and tested two different immunoassay formats (Figure 1B): an enzyme-linked immunosorbent assay (ELISA)-like format, which we named CRISPR-based immunosensing assay (CIA), and a magnetic bead (MB) assay, referred to as CRISPR-based immunomagnetic assay (CIMA). We optimized these assays to detect SARS-CoV-2 capsid protein antigens (spike S) in saliva samples, demonstrating superior sensitivity compared with a benchmark ELISA. This strategy expands the range of molecular targets detectable using CRISPR systems by employing Ab−DNA conjugates as activators of Cas12a.

2. RESULTS AND DISCUSSION

2.1. Collateral Cleavage Activity of Cas12a Triggered by an Antibody−DNA Conjugate. To study Ab−DNA conjugates as alternative synthetic activators of CRISPR-Cas12a, we first performed collateral cleavage studies using an Ab−DNA conjugate as CRISPR-Cas12a input. To do so, we produced the bioconjugate by covalently linking a 5′-DBCO-TEG-modified single-stranded DNA (ssDNA, 57 nt), previously activated with a cross-linker agent (PEG-NHS ester), to the amine groups of an anti-rabbit IgG (1 h, at 25 °C). Then, the Ab−DNA conjugate product was purified from unreacted reagents through ion exchange chromatography (proFIRE system, data not shown). The integrity of the Ab−DNA conjugate at the end of the process was confirmed by SDS-PAGE gel (Figure S1 in the Supporting Information). To

https://doi.org/10.1021/acssynbio.4c00541
ACS Synth. Biol. XXXX, XXX, XXX−XXX

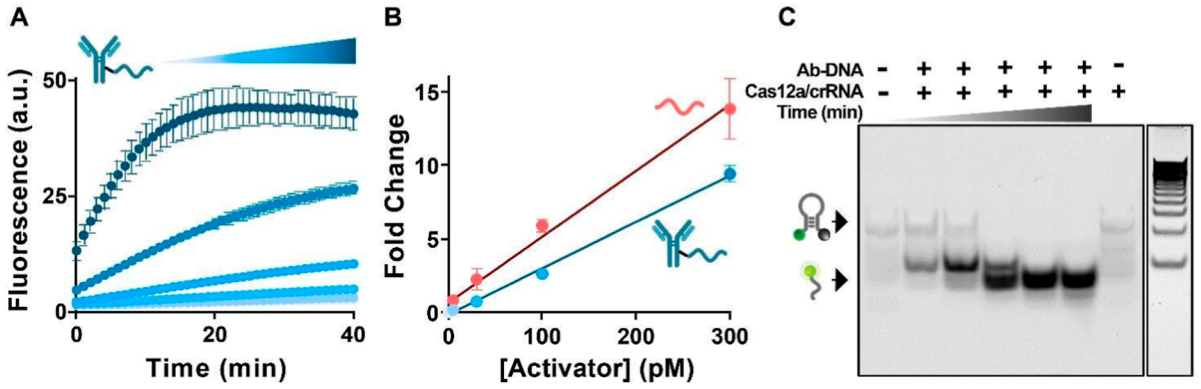

Figure 2. Collateral cleavage activity of CRISPR-Cas12a induced by antibody−DNA (Ab−DNA) conjugates. (A) Kinetic profiles of collateral activity triggered by different concentrations of the Ab−DNA conjugate (5 to 300 pM) using FRET-based DNA hairpin as a signal reporter. (B) Calibration curves reporting the signal transduction due to the collateral cleavage activity of Cas12a in the presence of a complementary DNA free in solution (red line) and the corresponding Ab−DNA conjugate (blue line). These experiments were conducted at 37 °C by adding the Cas12a reaction mix (250 nM of FRET-based DNA reporter and 20 nM of RNP complex) to the buffer solution containing different concentrations of the activator (ssDNA or Ab−DNA). Error bars in panels (A,B) reflect the standard deviation of three independent replicate experiments. (C) SDS-PAGE assay showing collateral cleavage activity induced by Ab−DNA over time. For further details about the experimental procedure, see the Supporting Information.

evaluate the effects of the bioconjugation on CRISPR-Cas12a collateral activity, we performed fluorimetric cleavage assays using different concentrations of Ab−DNA (from 5 to 300 pM) in the presence of a fixed concentration of the CRISPR-Cas12a complex (RNP, 20 nM) and a fixed concentration of the FRET-based DNA hairpin reporter (100 nM).[43] As the signal output of the immunoassay is generated upon binding of the bioconjugated ssDNA to the RNP, the crRNA sequence used in the assay is designed to be complementary (20 nt). The kinetic profiles show an increase of fluorescence over time at all the tested concentrations, demonstrating that the bioconjugated DNA strand is recognized by the RNP complex and is able to trigger the collateral activity of Cas12a also when covalently linked to the antibody (Figures 2A and S2).

Then, we compared the sensitivity of the system triggered by the Ab−DNA conjugate to that obtained with the same ssDNA sequence free in solution (Figure 2B). The calibration curves indicate that the sensitivity of the preamplification-free Cas12a-based detection systems is slightly higher for the free ssDNA in solution [limit of detection (LOD) = 1 pM] compared to that obtained using Ab−DNA as an activator (LOD = 12 pM) (Figure 2B).[44] However, the small difference can be likely explained by the steric hindrance effect of the antibody, which affects the recognition process between the RNP and the ssDNA (Figure 2B). Then, we also monitored the collateral cleavage activity induced by the Ab−DNA activator at different reaction times using SDS-PAGE analysis. The left lane in the gel displayed in Figure 2C contains a faint band at the highest molecular weight position, which corresponds to the intact FRET-based DNA reporter in the absence of Ab−DNA and the RNP complex. This low intensity is likely due to the highly quenched state of the hairpin; Notably, the stem structure brings the 3′ end with the FAM fluorophore and the 5′ end with the BHQ-1 quencher into close proximity, optimizing the FRET process. Upon adding the RNP (20 nM) and Ab−DNA (1 nM), the DNA reporter undergoes cleavage, resulting in the formation of shorter free fragments (lower M_w bands), which emit brighter fluorescence since the fluorophore and quencher are not held together anymore. As the reaction time in the presence of Ab−DNA increases, a higher degree of cleaving activity is observed. This is evidenced by the transition from the intact reporter (higher M_w bands) to the cleaved products (lower M_w bands) in lanes 2 through 6, corresponding to increasing reaction times.

2.2. Enhanced Sensitivity of the CRISPR-Based Immunosensing Assay (CIA) for the Detection of SARS-CoV-2. As our first test bed, we integrated Cas12a-based signal transduction into a sandwich-like ELISA (CIA) to detect SARS-CoV-2 spike S protein. To that end, a 96-well plate was coated with a mouse monoclonal anti-SARS-CoV-2 spike S antibody (capture antibody) and blocked with 2% BSA to prevent nonspecific absorption. Next, spike S protein was serially diluted in phosphate buffered saline (PBS) buffer, and detection antibodies were sequentially added and incubated at 37 °C, accompanied by rounds of washing to remove unbound reagents. As detection antibodies, a rabbit polyclonal anti-SARS-CoV-2 spike S IgG and an anti-rabbit IgG labeled with the ssDNA (Ab−DNA) were used. The optimization of antibody concentrations is detailed in the Supporting Information (Figures S3 and S4), along with the validation of the antibody pair for a sandwich detection assay (Figure S5). The immunoassay led to the formation of the antibody−antigen−antibody−(Ab−DNA) detection complex. To generate the signal output, the CRISPR reaction mix (20 nM RNP + 100 nM DNA reporter) was added, and fluorescence kinetics was measured over time. This confirmed that the Ab−DNA successfully activated Cas12a, enabling the detection of SARS-CoV-2 spike S proteins in the immunoassay format (Figure 3B).

Using fluorescence values obtained after 15 min of reaction at 37 °C, we generated the binding curve (Figure 3C). This method showed a linear response over the logarithm of spike S concentration ranging from 0.05 to 2.15 μg/mL, with a LOD of 2 ng/mL (Figure 3C, blue line). We also employed a standard commercial colorimetric ELISA kit to detect the same SARS-CoV-2 target through an immunosandwich assay (Figure 3C, purple line). Thanks to the multiple-turnover cleavage of the nucleic acid reporters and the intrinsic superior sensitivity of fluorescence, the developed assays show higher sensitivity compared to colorimetric assays. Indeed, compared to this commercial ELISA kit, our CRISPR-Cas12a assay demonstrated a lower limit of detection (2 ng/mL) versus the

https://doi.org/10.1021/acssynbio.4c00541
ACS Synth. Biol. XXXX, XXX, XXX−XXX

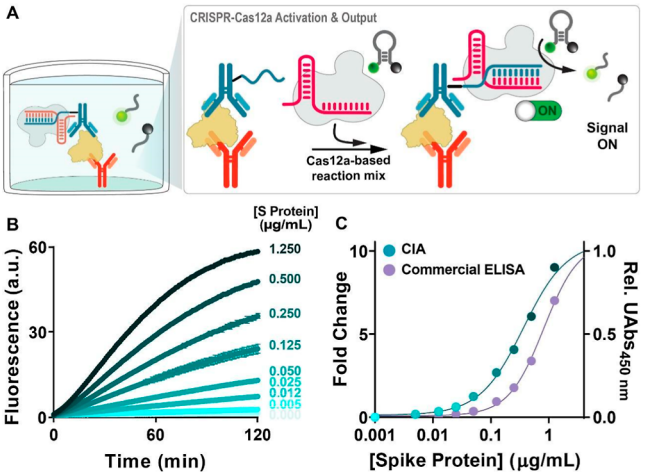

Figure 3. CRISPR-based immunosensing assay (CIA) for the detection of SARS-CoV-2. (A) Schematic representation of the CIA using Ab−DNA as activators of CRISPR-Cas12a signal transduction. (B) Kinetic profiles of CIA display the reporter cleavage over time at different spike protein concentrations in PBS buffer. (C) Calibration curves showing lower limits of detection for the detection of SARS-Co-2 V spike protein using CIA (blue curve, LOD = 2 ng/mL) with respect to a commercial ELISA kit (purple curve, LOD = 3.5 ng/mL) in buffer conditions. Error bars in the figure reflect the standard deviation of 3 replicate measurements; due to their small size in panel (C), the error bars cannot be distinguished from the dots.

commercial kit's (3.5 ng/mL). It is noteworthy that the commercial ELISA kit employs immunoreagents that are not specified by the manufacturer, meaning that our assay comparison may present an inherent bias due to the potential use of antibodies with superior affinities for the target. Nevertheless, it is reasonable to consider this bias minimal as manufacturers generally employ immunoreagents optimized for the best performance. Finally, our approach did not require any preamplification or enrichment steps as reported in previous publications using immuno-CRISPR detection.

2.3. CRISPR-Cas12a-Based Magnetic Bead Platform to Detect SARS-CoV-2 in Undiluted Saliva. Motivated by the above results, we decided to adapt this technology into a magnetoimmunoassay (CIMA). Magnetic beads offer several advantages, including their ease of manipulation using an external magnetic field, which facilitates washing and separation steps, thereby enhancing assay sensitivity and specificity (Figure 4A).[45−47] We immobilized the mouse monoclonal anti-SARS-CoV-2 antibody onto the surface of the beads to ensure selective capture of the target protein from the sample and equimolar concentration of rabbit polyclonal anti-SARS-CoV-2 spike S IgG and an anti-rabbit IgG labeled with oligonucleotide (Ab−DNA) to allow the formation of the immunocomplex. In our immunoassay, the target is sandwiched between the immobilized antibodies on the beads and the Ab−DNA conjugates. After the formation of the immunocomplex, the beads are washed to remove any unbound components. By adding the Cas12a reaction mix to the solution, the fluorescence signal change over time indicates that the CIMA detection assay worked successfully, showing a good sensitivity in the buffer (LOD = 54 ng/mL, Figure S6).

To further investigate the CIMA method for protein analysis in complex matrices, we tested CIMA in undiluted human saliva samples. Specifically, we added known concentrations of

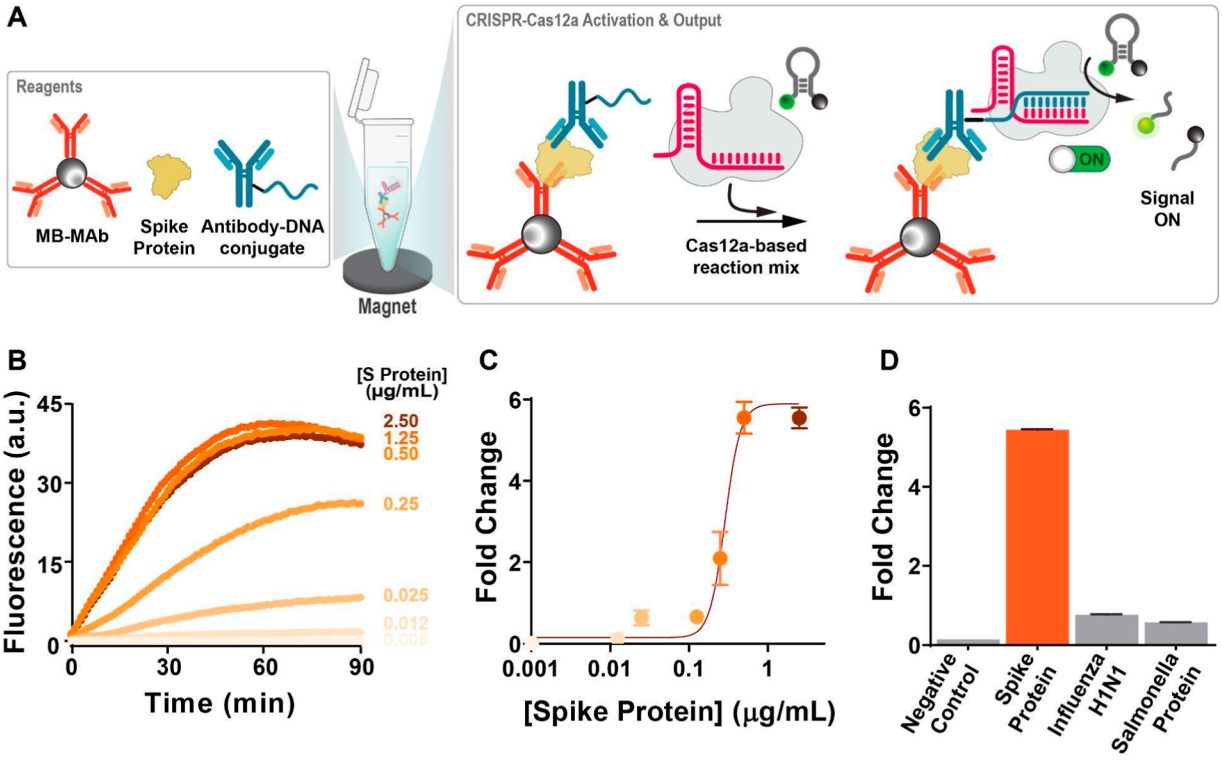

Figure 4. (A) Schematic description of the CRISPR-based immunomagnetic assay (CIMA). (B) Kinetic profiles of collateral cleavage activity in the presence of SARS-CoV-2 spike S protein spiked in human saliva. (C) Calibration curve of the CIMA over different target concentrations. (D) To validate the specificity of the developed platform, we tested saliva samples spiked with nonspecific pathogens. Error bars in the figure reflect the standard deviation of 3 replicate measurements.

https://doi.org/10.1021/acssynbio.4c00541
ACS Synth. Biol. XXXX, XXX, XXX−XXX

protein spike to undiluted saliva (see Materials and Methods). The fluorescence kinetic profiles and the binding curve in Figure 4B,C clearly confirm that the method is not significantly affected by matrix effects (LOD = 70 ng/mL and a linear response over the logarithm of spike S concentration ranging from 0.16 to 0.45 μg/mL). The assay is also highly specific as saliva samples spiked with nonspecific proteins do not generate significant changes in fluorescence output. In addition, it is important to highlight that the total analysis time for the proposed CIMA is 1 h and 45 min including all washing steps. In contrast, a commercial sandwich ELISA with a colorimetric readout would require a higher number of incubation/washing steps, resulting in a total time of approximately 4 h. Besides, the use of magnetic beads in suspension as the support provides faster and more efficient mixing that enhances the assay's sensibility compared to sandwich ELISAs.

2.4. Conclusions and Perspectives of CRISPR-Based Immunoassays. Here, we developed two immunoassay platforms that exploit CRISPR-Cas12 for the detection of non-nucleic acid targets. To achieve this, we modified a recognition element, an anti-IgG antibody, with a single-stranded DNA (ssDNA) strand that can be targeted by the CRISPR-Cas12a ribonucleoprotein (RNP) complex, triggering its collateral nonspecific nuclease activity. We demonstrated that the bioconjugate preserved its capability to trigger the CRISPR-Cas12a collateral activity. Next, we demonstrated that Ab−DNA can be used as a labeled recognition element in ELISA-like immunoassays (i.e. CRISPR-based immunosensing assay, CIA). Specifically, we successfully detected a disease biomarker, SARS-CoV-2 spike S protein, with a limit of detection (LOD) better than commercial ELISA kits in a simple, straightforward ELISA-like assay without the need for nucleic acid amplification steps in the sample. Then, we deployed the system in a magnetic immunosandwich assay format (i.e. CRISPR-based immunomagnetic assay, CIMA), resulting in a quick and user-friendly test for the detection of SARS-CoV-2 in undiluted saliva samples with high specificity over other disease biomarkers.

The proposed CRISPR-Cas12 immunoassay platforms fulfill most of the criteria necessary for producing a sensitive, inexpensive, and easily performed immunoassay. The fluorescence signal transduction allows for the use of specific excitation and emission wavelengths, which minimizes interference from other sample components, making the assay both sensitive and accurate. One key advantage is the minimal likelihood of nonspecific reactions generating background fluorescent signals after the washing step. DNA reporters are particularly suitable substrates due to their stability over a wide range of conditions and easy preservation and storage, either lyophilized at room temperature or when solubilized at −20 °C, for long-term periods (months to years). In contrast, other substrates for ELISA assays, such as TMB, 4-MUP, and luminol, often require specific conditions (e.g., storage at 4 °C in strict darkness) to maintain stability for just a few months. In the realm of luminescent immunoassays, luminol is popular due to its intense and prolonged light emission (2 to 20 min) and low background. However, "home-brew" preparations of luminol require careful pH stabilization to ensure optimal oxidase activity and light emission. Alkaline phosphatase and galactosidase each have preferred luminescent substrates (AMPPD and AMPGD, respectively) that require enhancers and specific buffers for improved performance. Furthermore, uncontrolled oxidizing reactions can process these substrates into signaling products, complicating the assay. In contrast, FRET-based DNA reporters perform well in buffer solutions at physiological pH and do not suffer from significant stability issues. They exhibit mandatory features for suitable substrates: low background, intense and stable light emission in the active state, and consistent quality as commercial products. The specificity of the CRISPR-Cas12a system minimizes the likelihood of unwanted reactions, ensuring that the observed signal is primarily due to intended DNA cleavage.[48] Additionally, the selection of the CRISPR-Cas12a enzyme meets most of the essential criteria for producing a sensitive and easy-to-perform immune platform. Cas12a shows high stability at typical assay temperatures (4−37 °C), a high turnover rate, and its activity is almost unaffected by other biological components of the assay while maintaining a low cost. Indeed, one benefit of CRISPR-based diagnostic assays is that they do not rely on expensive and complex laboratory equipment. Cas enzymes and crRNAs can be quickly and efficiently produced in large quantities, reducing the dependency of CRISPR-based assays on supply chain issues. Furthermore, covalently attaching the ssDNA to the antibody renders the assay compact and modular, allowing it to operate as a standard immunoassay without any further pre- or postamplification steps, as the antibody already contains the ssDNA activator.

However, some issues still need to be addressed, including difficulties in sample processing and stability. The storage of solutions containing crRNA, cleavage reporter, and Cas protein typically requires ultralow-temperature freezers and lyophilization.[16,49] Although this industrial problem requires expertise in formulation development and process engineering, advancements in these areas could significantly enhance the practicality and widespread use of CRISPR-Cas12 immunoassay platforms. Overall, we believe that using the CRISPR-Cas12 enzyme in combination with the Ab−DNA conjugate and a DNA reporter as a substrate may represent an appropriate alternative for immunoassay development as all of the components meet most of the criteria necessary to produce a sensitive, low-cost, and easily performed immunoassay.

3. MATERIALS AND METHODS

3.1. Reagents and Materials. All reagents and oligonucleotide sequences are listed and detailed in the Supporting Information.

3.2. CIA for SARS-CoV-2 Spike S Protein Detection. CIA for the detection of spike S protein was performed following a standard ELISA protocol incorporating the CRISPR-Cas12a signal transduction and fluorescence reading for the target detection. Briefly, MaxiSorp black multiwell plates were coated by adding 50 μL of the monoclonal anti-spike S antibody as a capturing recognition element at 0.5 μg/mL, in 50 mM carbonate buffer at pH 9.0, and incubated at 4 °C overnight. Each step of incubation was proceeded by three washing steps in phosphate buffered saline (PBS) + 0.05% (v/v) Tween 20. First, to prevent nonspecific interactions, 200 μL of blocking solution (2% w/v BSA in PBS) was added to each well and incubated for 2 h at 37 °C. Second, 100 μL of sample containing the target (SARS-CoV-2 spike S protein) was added and incubated for 1 h at 37 °C. Following this, 100 μL of the unlabeled rabbit polyclonal anti-spike S antibody at 0.5 μg/mL in 1% w/v BSA and 0.05% v/v Tween 20 in PBS buffer was incubated for 1 h at 37 °C. Next, all wells with 100 μL of the goat polyclonal antirabbit IgG antibody labeled with ssDNA

https://doi.org/10.1021/acssynbio.4c00541
ACS Synth. Biol. XXXX, XXX, XXX−XXX

(Ab−DNA) at 0.5 μg/mL in 1% w/v BSA and 0.05% v/v Tween 20 in PBS buffer were incubated for 1 h at 37 °C. Finally, 30 μL of Cas12a/crRNA complex at 200 nM was added to each well and incubated for 30 min at 37 °C in the presence of 30 μL of hairpin reporter at 400 nM. The fluorescence signal was collected using an excitation wavelength of 490 nm and an emission wavelength of 525 nm. Unless otherwise stated, all measurements were performed in triplicates.

Enzyme-linked immunosorbent assays (ELISAs) as reference techniques for the detection of SARS-CoV-2 spike S protein were performed following the standard ELISA protocol for colorimetric detection.[50]

3.3. CIMA for SARS-CoV-2 Spike S Protein Detection. The magnetic beads (MBs) were modified with the capture antibody using 250 μL of MBs (4×10^8 particles/mL) and washed twice using 1 mL of PBS. Unless otherwise stated, each washing cycle consisted of retaining the MBs at the bottom of the Eppendorf through the action of a magnet and removing the supernatant with a micropipette by adding the washing buffer. The washed MBs were blocked by incubating in 1 mL of PBS containing 3% w/v BSA for 30 min at room temperature on a slow-rotating shaker. The MBs were then retrieved, the supernatant discarded, and the MBs were resuspended in 500 μL of PBS containing 10 μg of mouse anti-SARS-CoV-2 monoclonal antibody and incubated again for 30 min at room temperature with gentle rotation. Next, the MBs were washed twice with 1 mL of PBS, resuspended in 250 μL of 0.02% w/v NaN_3 PBS (storage buffer), and stored at 4 °C.

After three washing steps, the coated MBs were resuspended in PBS, and 10 μL of the antibody-modified MBs was added to 200 μL of sample, SARS-CoV-2 spike recombinant target protein in incubation buffer (1% w/v BSA and 0.05% v/v Tween 20 in PBS). Then, 200 μL containing a mix of polyclonal αSpike at 0.5 μg/mL and Ab−DNA at 0.5 μg/mL in incubation buffer was added to each sample. The samples were incubated for 60 min at room temperature. After an additional washing step, (2 times in 0.05% v/v Tween 20 PBS and once with 1 mL of PBS), the MBs were resuspended in 21 μL of TRIS buffer (10 mM Tris−HCl, 50 mM NaCl, and 10 mM $MgCl_2$ at pH = 7.9). Twenty μL of the resulting MB sample was mixed with 3 μL of crRNA/CRISPR-Cas12a ribonucleic complex (RNP) at 200 nM and incubated for 30 min at 37 °C. The resulting 23 μL was combined with 7 μL of DNA hairpin fluorescence reporter (final concentration: 200 nM) and incubated at 37 °C for 10 min. Finally, 25 μL of each final mix was added in a multiwell plate to perform the fluorescence measurement over time. Unless otherwise stated, all measurements were performed in triplicate.

3.4. Native Polyacrylamide Gel Electrophoresis (PAGE) Analysis of Collateral Cleavage Activity of Cas12a. Native PAGE 1.5 mm thickness gels were prepared at 18% polyacrylamide (29:1 acrylamide/bis(acrylamide)) in TBE 10× buffer (1 M Tris, 0.9 M boric acid, and 0.01 M EDTA) at pH 8.3. A gel solution was prepared by mixing 5.7 mL of distilled water, 4.1 mL of TBE 10× buffer, 4.2 mL of 40% acrylamide/bis(acrylamide) solution, 75 μL of 10% (w/v) ammonium persulfate (APS), and 14 μL of TEMED. The solution was stirred to ensure its homogeneity and cast into the glass plates. The gel glass plates were sealed with a 10-well comb to create the lanes and allowed to polymerize. Samples were prepared by mixing 1 μL of 60% w/w glycerol with 10 μL of sample, and then the mixture was loaded into its corresponding well. O'range Ruler 5 base pair DNA ladder was used as the DNA standard. The samples were prepared by adding, to a 1 nM solution of Ab−DNA, the Cas12a/crRNA enzymatic complex and the DNA hairpin reporter to final concentrations of 20 and 250 nM, respectively, both previously pretreated as described in the section "Preparation of the CRISPR-Cas12a Detection System". The reactions were halted at increasing time intervals (0, 15, 30, 60, and 120 min) by heating the solutions to 65 °C for 10 min to deactivate the Cas12a enzyme. Native PAGE was carried out in a Mini-PROTEAN tetra cell unit (Bio-Rad) for electrophoresis. The samples were run for 80 min at a constant voltage of 120 V at room temperature using TBE 1× (pH 8.3, 0.1 M Tris, 0.09 M boric acid, and 0.001 EDTA) as the running buffer. Gels were scanned in a ChemiDoc imaging system (Bio-Rad) using filters for FAM emission. The same gels were imaged after 30 min of SYBR gold staining dissolved in TBE 1× buffer at pH 8.3 to visualize the ladder signal.

3.5. Data Analysis. Unless otherwise specified, signal gains were calculated as fold change using the fluorescent value obtained at 15 min right after the addition of the Cas12a-based reaction mix. This parameter represents the relative change in the fluorescence signal associated with the trans-cleavage activity of Cas12a in the presence vs in the absence of target. The fold change is calculated using the following expression

$$\text{fold change} = \frac{F_{\text{target}} - F_0}{F_0}$$

where F_{target} is the fluorescence signal observed in the presence of target (SARS-CoV-2 spike protein) and F_0 corresponds to the background fluorescence signal obtained in the absence of target.

The fold change vs target concentration was fitted using the 4-parameter expression

$$\text{signal} = S_m + \frac{(S_0 - S_m)}{\left[1 + \left(\frac{[T]}{K_d}\right)^{n_H}\right]}$$

where S_0 corresponds to the minimum signal value, S_m to the maximum signal value, T the target's concentration, K_d the dissociation constant, and n_H the hill coefficient.

The limits of detection (LODs) for collateral cleavage activity calibration curves were calculated based on the ratio of 3 times the standard deviation of the blank divided by the slope of the linear response concentration range. The LOD for binding curves was calculated as the sum of the blank mean plus 3 times the standard deviation of the blank.

The linear ranges were determined as the concentration windows that encompass the transition from 10% to 90% relative signal changes in the binding curves.

Further experimental procedures and parameters are detailed in the Supporting Information.

■ ASSOCIATED CONTENT

Supporting Information

The Supporting Information is available free of charge at https://pubs.acs.org/doi/10.1021/acssynbio.4c00541.

Reagents and materials; additional experimental details and procedures; PAGE gels of the Ab−DNA, ELISA, CIA, and CIMA optimizations; standard commercial ELISA; and CIMA challenged in buffer (PDF)

https://doi.org/10.1021/acssynbio.4c00541
ACS Synth. Biol. XXXX, XXX, XXX−XXX

AUTHOR INFORMATION

Corresponding Authors

Alejandro Chamorro-Garcia − *Department of Chemical Science and Technologies, University of Rome Tor Vergata, 00133 Rome, Italy*; Email: alejandro.chamorro.garcia@uniroma2.it

Alessandro Porchetta − *Department of Chemical Science and Technologies, University of Rome Tor Vergata, 00133 Rome, Italy*; orcid.org/0000-0002-4061-5574; Email: alessandro.porchetta@uniroma2.it

Authors

Elisa Paialunga − *Department of Chemical Science and Technologies, University of Rome Tor Vergata, 00133 Rome, Italy*

Neda Bagheri − *Department of Chemical Science and Technologies, University of Rome Tor Vergata, 00133 Rome, Italy*; orcid.org/0009-0005-0805-8201

Marianna Rossetti − *Department of Chemical Science and Technologies, University of Rome Tor Vergata, 00133 Rome, Italy*

Laura Fabiani − *Department of Chemical Science and Technologies, University of Rome Tor Vergata, 00133 Rome, Italy*

Laura Micheli − *Department of Chemical Science and Technologies, University of Rome Tor Vergata, 00133 Rome, Italy*

Complete contact information is available at: https://pubs.acs.org/10.1021/acssynbio.4c00541

Author Contributions

E.P. designed and performed experimental work, analyzed data, and participated in writing the manuscript. N.B. and M.R. performed part of experimental work. L.F. and L.M. assisted in the conceptualization and research design. A.C-G. performed experimental work, data analysis, and participated in the manuscript writing. A.P. conceived, designed, and directed the study, analyzed and interpreted data, and wrote the manuscript.

Notes

The authors declare no competing financial interest.

ACKNOWLEDGMENTS

The research leading to these results has received funding from AIRC under MFAG 2022—ID. 27151 project—P.I. Porchetta Alessandro. A.P. acknowledges funding from the Italian Ministry of University and Research (Project of National Interest, PRIN, 2022FPYZ2N). This project has received funding from the European Union—NextGenerationEU under the program YOUNG RESEARCHER—MSCA (Project ID: MSCA_0000010). M.R. was supported from a Fondazione Umberto Veronesi postdoctoral fellowship.

REFERENCES

(1) Kaminski, M. M.; Abudayyeh, O. O.; Gootenberg, J. S.; Zhang, F.; Collins, J. J. CRISPR-Based Diagnostics. *Nat. Biomed. Eng.* **2021**, *5* (7), 643−656.

(2) Li, S.-Y.; Cheng, Q.-X.; Wang, J.-M.; Li, X.-Y.; Zhang, Z.-L.; Gao, S.; Cao, R.-B.; Zhao, G.-P.; Wang, J. CRISPR-Cas12a-Assisted Nucleic Acid Detection. *Cell Discov.* **2018**, *4*, 20.

(3) Kellner, M. J.; Koob, J. G.; Gootenberg, J. S.; Abudayyeh, O. O.; Zhang, F. SHERLOCK: Nucleic Acid Detection with CRISPR Nucleases. *Nat. Protoc.* **2019**, *14* (10), 2986−3012.

(4) Gootenberg, J. S.; Abudayyeh, O. O.; Lee, J. W.; Essletzbichler, P.; Dy, A. J.; Joung, J.; Verdine, V.; Donghia, N.; Daringer, N. M.; Freije, C. A.; Myhrvold, C.; Bhattacharyya, R. P.; Livny, J.; Regev, A.; Koonin, E. V.; Hung, D. T.; Sabeti, P. C.; Collins, J. J.; Zhang, F. Nucleic Acid Detection with CRISPR-Cas13a/C2c2. *Science* **2017**, *356* (6336), 438−442.

(5) Huang, Z.; Lyon, C. J.; Wang, J.; Lu, S.; Hu, T. Y. CRISPR Assays for Disease Diagnosis: Progress to and Barriers Remaining for Clinical Applications. *Adv. Sci.* **2023**, *10* (20), 2301697.

(6) Yang, S.; Zhou, L.; Fang, Z.; Wang, Y.; Zhou, G.; Jin, X.; Cao, Y.; Zhao, J. Proximity-Guaranteed DNA Machine for Accurate Identification of Breast Cancer Extracellular Vesicles. *ACS Sens.* **2024**, *9* (4), 2194−2202.

(7) Li, Q.-N.; Ma, A.-X.; Wang, D.-X.; Dai, Z.-Q.; Wu, S.-L.; Lu, S.; Zhu, L.; Jiang, H.-X.; Pang, D.-W.; Kong, D.-M. Allosteric Activator-Regulated CRISPR/Cas12a System Enables Biosensing and Imaging of Intracellular Endogenous and Exogenous Targets. *Anal. Chem.* **2024**, *96* (16), 6426−6435.

(8) Li, T.; Cheng, N. Sensitive and Portable Signal Readout Strategies Boost Point-of-Care CRISPR/Cas12a Biosensors. *ACS Sens.* **2023**, *8* (11), 3988−4007.

(9) Wang, T.; Wang, Z.; Bai, L.; Zhang, X.; Feng, J.; Qian, C.; Wang, Y.; Wang, R. Next-Generation CRISPR-Based Diagnostic Tools for Human Diseases. *TrAC, Trends Anal. Chem.* **2023**, *168*, 117328.

(10) Huang, T.; Zhang, R.; Li, J. CRISPR-Cas-Based Techniques for Pathogen Detection: Retrospect, Recent Advances, and Future Perspectives. *J. Adv. Res.* **2023**, *50*, 69−82.

(11) Chen, Y.; Mei, Y.; Jiang, X. Universal and High-Fidelity DNA Single Nucleotide Polymorphism Detection Based on a CRISPR/Cas12a Biochip. *Chem. Sci.* **2021**, *12* (12), 4455−4462.

(12) Li, M.; Yin, F.; Song, L.; Mao, X.; Li, F.; Fan, C.; Zuo, X.; Xia, Q. Nucleic Acid Tests for Clinical Translation. *Chem. Rev.* **2021**, *121* (17), 10469−10558.

(13) Soleimany, A. P.; Bhatia, S. N. Activity-Based Diagnostics: An Emerging Paradigm for Disease Detection and Monitoring. *Trends. Mol. Med.* **2020**, *26* (5), 450−468.

(14) Hao, L.; Zhao, R. T.; Welch, N. L.; Tan, E. K. W.; Zhong, Q.; Harzallah, N. S.; Ngambenjawong, C.; Ko, H.; Fleming, H. E.; Sabeti, P. C.; Bhatia, S. N. CRISPR-Cas-Amplified Urinary Biomarkers for Multiplexed and Portable Cancer Diagnostics. *Nat. Nanotechnol.* **2023**, *18* (7), 798−807.

(15) Liu, H.; Dong, J.; Duan, Z.; Xia, F.; Willner, I.; Huang, F. Light-Activated CRISPR-Cas12a for Amplified Imaging of microRNA in Cell Cycle Phases at Single-Cell Levels. *Sci. Adv.* **2024**, *10* (30), No. eadp6166.

(16) Ghouneimy, A.; Mahas, A.; Marsic, T.; Aman, R.; Mahfouz, M. CRISPR-Based Diagnostics: Challenges and Potential Solutions toward Point-of-Care Applications. *ACS Synth. Biol.* **2023**, *12* (1), 1−16.

(17) Liu, F. X.; Cui, J. Q.; Wu, Z.; Yao, S. Recent Progress in Nucleic Acid Detection with CRISPR. *Lab Chip* **2023**, *23* (6), 1467−1492.

(18) Bruch, R.; Urban, G. A.; Dincer, C. CRISPR/Cas Powered Multiplexed Biosensing. *Trends Biotechnol.* **2019**, *37* (8), 791−792.

(19) Ackerman, C. M.; Myhrvold, C.; Thakku, S. G.; Freije, C. A.; Metsky, H. C.; Yang, D. K.; Ye, S. H.; Boehm, C. K.; Kosoko-Thoroddsen, T.-S. F.; Kehe, J.; Nguyen, T. G.; Carter, A.; Kulesa, A.; Barnes, J. R.; Dugan, V. G.; Hung, D. T.; Blainey, P. C.; Sabeti, P. C. Massively Multiplexed Nucleic Acid Detection with Cas13. *Nature* **2020**, *582* (7811), 277−282.

(20) Johnston, M.; Ceren Ates, H.; Glatz, R. T.; Mohsenin, H.; Schmachtenberg, R.; Göppert, N.; Huzly, D.; Urban, G. A.; Weber, W.; Dincer, C. Multiplexed Biosensor for Point-of-Care COVID-19 Monitoring: CRISPR-Powered Unamplified RNA Diagnostics and Protein-Based Therapeutic Drug Management. *Mater. Today* **2022**, *61*, 129−138.

(21) Del Giovane, S.; Bagheri, N.; Di Pede, A. C.; Chamorro, A.; Ranallo, S.; Migliorelli, D.; Burr, L.; Paoletti, S.; Altug, H.; Porchetta, A. Challenges and Perspectives of CRISPR-Based Technology for

Diagnostic Applications. *TrAC, Trends Anal. Chem.* **2024**, *172*, 117594.
(22) Shen, J.; Zhou, X.; Shan, Y.; Yue, H.; Huang, R.; Hu, J.; Xing, D. Sensitive Detection of a Bacterial Pathogen Using Allosteric Probe-Initiated Catalysis and CRISPR-Cas13a Amplification Reaction. *Nat. Commun.* **2020**, *11* (1), 267.
(23) Cheng, X.; Li, Y.; Kou, J.; Liao, D.; Zhang, W.; Yin, L.; Man, S.; Ma, L. Novel Non-Nucleic Acid Targets Detection Strategies Based on CRISPR/Cas Toolboxes: A Review. *Biosens. Bioelectron.* **2022**, *215*, 114559.
(24) Zhou, J.; Ren, X.; Wang, X.; Li, Z.; J Xian, C. Recent Advances and Challenges of the Use of the CRISPR/Cas System as a Non-Nucleic Acid Molecular Diagnostic. *Heliyon* **2023**, *9* (12), No. e22767.
(25) Chen, Y.; Wu, H.; Qian, S.; Yu, X.; Chen, H.; Wu, J. Applying CRISPR/Cas System as a Signal Enhancer for DNAzyme-Based Lead Ion Detection. *Anal. Chim. Acta* **2022**, *1192*, 339356.
(26) Peng, L.; Zhou, J.; Liu, G.; Yin, L.; Ren, S.; Man, S.; Ma, L. CRISPR-Cas12a Based Aptasensor for Sensitive and Selective ATP Detection. *Sens. Actuat. B* **2020**, *320*, 128164.
(27) Li, Q.; Li, X.; Zhou, P.; Chen, R.; Xiao, R.; Pang, Y. Split Aptamer Regulated CRISPR/Cas12a Biosensor for 17β-Estradiol through a Gap-Enhanced Raman Tags Based Lateral FLow Strategy. *Biosens. Bioelectron.* **2022**, *215*, 114548.
(28) Li, Y.; Mansour, H.; Watson, C. J. F.; Tang, Y.; MacNeil, A. J.; Li, F. Amplified Detection of Nucleic Acids and Proteins Using an Isothermal Proximity CRISPR Cas12a Assay. *Chem. Sci.* **2021**, *12* (6), 2133−2137.
(29) Ranallo, S.; Porchetta, A.; Ricci, F. DNA-Based Scaffolds for Sensing Applications. *Anal. Chem.* **2019**, *91* (1), 44−59.
(30) Bagheri, N.; Chamorro, A.; Idili, A.; Porchetta, A. PAM-Engineered Toehold Switches as Input-Responsive Activators of CRISPR-Cas12a for Sensing Applications. *Angew. Chem., Int. Ed.* **2024**, *63*, No. e202319677.
(31) Engelen, W.; Zhu, K.; Subedi, N.; Idili, A.; Ricci, F.; Tel, J.; Merkx, M. Programmable Bivalent Peptide−DNA Locks for pH-Based Control of Antibody Activity. *ACS Cent. Sci.* **2020**, *6* (1), 22−31.
(32) Dovgan, I.; Koniev, O.; Kolodych, S.; Wagner, A. Antibody−Oligonucleotide Conjugates as Therapeutic, Imaging, and Detection Agents. *Bioconjugate Chem.* **2019**, *30* (10), 2483−2501.
(33) Bezerra, A. B.; Kurian, A. S. N.; Easley, C. J. Nucleic-Acid Driven Cooperative Bioassays Using Probe Proximity or Split-Probe Techniques. *Anal. Chem.* **2021**, *93* (1), 198−214.
(34) Malou, N.; Raoult, D. Immuno-PCR: a promising ultrasensitive diagnostic method to detect antigens and antibodies. *Trends Microbiol.* **2011**, *19* (6), 295−302.
(35) Märcher, A.; Nijenhuis, M. A. D.; Gothelf, K. V. A Wireframe DNA Cube: Antibody Conjugate for Targeted Delivery of Multiple Copies of Monomethyl Auristatin E. *Angew. Chem., Int. Ed.* **2021**, *60* (40), 21691−21696.
(36) Schnitzbauer, J.; Strauss, M. T.; Schlichthaerle, T.; Schueder, F.; Jungmann, R. Super-Resolution Microscopy with DNA-PAINT. *Nat. Protoc.* **2017**, *12* (6), 1198−1228.
(37) Baranda Pellejero, L.; Nijenhuis, M. A. D.; Ricci, F.; Gothelf, K. V. Protein-Templated Reactions Using DNA-Antibody Conjugates. *Small* **2023**, *19* (13), 2200971.
(38) Sela, T.; Mansø, M.; Siegel, M.; Marban-Doran, C.; Ducret, A.; Niewöhner, J.; Ravn, J.; Martin, R. E.; Sommer, A.; Lohmann, S.; Krippendorff, B.-F.; Ladefoged, M.; Indlekofer, A.; Quaiser, T.; Bueddefeld, F.; Koller, E.; Mohamed, M. Y.; Oelschlaegel, T.; Gothelf, K. V.; Hofer, K.; Schumacher, F. F. Diligent Design Enables Antibody-ASO Conjugates with Optimal Pharmacokinetic Properties. *Bioconjugate Chem.* **2023**, *34* (11), 2096−2111.
(39) Lee, I.; Kwon, S.-J.; Heeger, P.; Dordick, J. S. Ultrasensitive ImmunoMag-CRISPR Lateral Flow Assay for Point-of-Care Testing of Urinary Biomarkers. *ACS Sens.* **2024**, *9* (1), 92−100.
(40) Lee, I.; Kwon, S.-J.; Sorci, M.; Heeger, P. S.; Dordick, J. S. Highly Sensitive Immuno-CRISPR Assay for CXCL9 Detection. *Anal. Chem.* **2021**, *93* (49), 16528−16534.
(41) Chen, Q.; Tian, T.; Xiong, E.; Wang, P.; Zhou, X. CRISPR/Cas13a Signal Amplification Linked Immunosorbent Assay for Femtomolar Protein Detection. *Anal. Chem.* **2020**, *92* (1), 573−577.
(42) Li, Y.; Deng, F.; Goldys, E. M. A Simple and Versatile CRISPR/Cas12a-Based Immunosensing Platform: Towards Attomolar Level Sensitivity for Small Protein Diagnostics. *Talanta* **2022**, *246*, 123469.
(43) Rossetti, M.; Merlo, R.; Bagheri, N.; Moscone, D.; Valenti, A.; Saha, A.; Arantes, P. R.; Ippodrino, R.; Ricci, F.; Treglia, I.; Delibato, E.; van der Oost, J.; Palermo, G.; Perugino, G.; Porchetta, A. Enhancement of CRISPR/Cas12a *Trans* -Cleavage Activity Using Hairpin DNA Reporters. *Nucleic Acids Res.* **2022**, *50* (14), 8377−8391.
(44) Feng, W.; Zhang, H.; Le, X. C. Signal Amplification by the *Trans* -Cleavage Activity of CRISPR-Cas Systems: Kinetics and Performance. *Anal. Chem.* **2023**, *95* (1), 206−217.
(45) Fabiani, L.; Saroglia, M.; Galatà, G.; De Santis, R.; Fillo, S.; Luca, V.; Faggioni, G.; D'Amore, N.; Regalbuto, E.; Salvatori, P.; Terova, G.; Moscone, D.; Lista, F.; Arduini, F. Magnetic Beads Combined with Carbon Black-Based Screen-Printed Electrodes for COVID-19: A Reliable and Miniaturized Electrochemical Immunosensor for SARS-CoV-2 Detection in Saliva. *Biosens. Bioelectron.* **2021**, *171*, 112686.
(46) Toyos-Rodríguez, C.; Llamedo-González, A.; Pando, D.; García, S.; García, J. A.; García-Alonso, F. J.; De La Escosura-Muñiz, A. Novel Magnetic Beads with Improved Performance for Alzheimer's Disease Biomarker Detection. *Microchem. J.* **2022**, *175*, 107211.
(47) Jamshaid, T.; Neto, E. T. T.; Eissa, M. M.; Zine, N.; Kunita, M. H.; El-Salhi, A. E.; Elaissari, A. Magnetic Particles: From Preparation to Lab-on-a-Chip, Biosensors, Microsystems and Microfluidics Applications. *TrAC, Trends Anal. Chem.* **2016**, *79*, 344−362.
(48) Gibbs, J. *Selecting the Detection System—Colorimetric, Fluorescent, Luminiscent Methods—ELISA Technical Bulletin-No. 5*, 2001.
(49) Li, H.; Xie, Y.; Chen, F.; Bai, H.; Xiu, L.; Zhou, X.; Guo, X.; Hu, Q.; Yin, K. Amplification-Free CRISPR/Cas Detection Technology: Challenges, Strategies, and Perspectives. *Chem. Soc. Rev.* **2023**, *52* (1), 361−382.
(50) ELISA protocol Thermofisher. https://www.thermofisher.com/it/en/home/references/protocols/cell-and-tissue-analysis/elisa-protocol/general-elisa-protocol.html (accessed July 07, 2024).

https://doi.org/10.1021/acssynbio.4c00541
ACS Synth. Biol. XXXX, XXX, XXX−XXX